Chem Soc Rev

Catalytically active gold on ordered titania supports†

Mingshu Chen[ab] and D. Wayne Goodman*[a]

Almost two decades have passed since supported Au nanoparticles were found to be active for CO oxidation. This discovery inspired extensive research addressing the origin of the unique properties of supported Au nanoparticles, the design and synthesis of potentially technical Au catalysts, and the extension of Au catalysis to other reactions. This *tutorial review* summarises the current understanding of the origin of the unique properties of titania-supported Au catalysts for carbon monoxide oxidation. The key issues of catalysis by nanostructured Au, effects of oxide support and active site/structure, especially those provided from model studies are discussed in detail. The successful synthesis of a highly catalytically active gold bilayer may lead to the design and synthesis of practically active Au nanofilm catalysts.

1. Introduction

Au is a highly inert metal that historically has been considered to be catalytically inactive. However early investigations showed Au to have significant catalytic activity for certain reactions, *e.g.* hydrogenation of olefins over supported Au by Bond *et al.* in 1973,[1] although not with activity comparable to other metals. In 1987 Haruta *et al.* made the surprising discovery[2] that Au supported on reducible oxide supports exhibited novel catalytic activity for CO oxidation. This report stimulated considerable interest in Au as a catalyst such that Au catalysis is currently one of the most active areas in catalytic science. Au has been shown to be an active catalyst for a number of reactions including CO oxidation,

hydrogenation, and selective oxidation, a topic that has been thoroughly reviewed recently by Hashmi and Hutchings.[3]

The unique catalytic properties of supported nanosized-Au particles depend strongly on the support, particle size and shape, as well as other factors.[2,4,5] Numerous studies have addressed how the shape, structure, and electronic properties of the Au particles correlate with the catalytic activity. For example, the size of the Au nanoparticles and the properties of the support have been shown to be critical in giving rise to the unique catalytic activity. Furthermore, active sites have been proposed to reside at the interface between the Au nanoparticles and the oxide support. However, the size distribution and shapes of nanoparticles in oxide-supported catalysts often vary widely, and the particle structure, particularly the structure at the metal–oxide interface, are generally not well-defined. Moreover, Au nanoparticles typically sinter rapidly under reaction conditions.[4] Because of these complexities the active site/structure of supported Au catalysts remain unclear. The recent synthesis of highly ordered Au mono- and bi-layer structures or "nanofilms" supported on a highly reduced and ordered titania surface and the exceptionally high catalytic

[a] Department of Chemistry, Texas A&M University, College Station, TX 77842-3012, USA
[b] State Key Laboratory of Physical Chemistry of Solid Surface, Department of Chemistry, Xiamen University, Fujian, Xiamen 361005, China
† Part of a thematic issue covering the topic of gold: chemistry, materials and catalysis.

Mingshu Chen received his BS in Applied Chemistry from Chengdu University of Science and Technology, a MD in 1994 and a PhD in 1997 from Xiamen University in Catalysis, where he subsequently served as a research associate/lecturer. In 2002 he earned a PhD (Surface Science) from Kyushu University and shortly thereafter joined the research group of Prof. Goodman at Texas A&M University. In 2007 he joined the faculty of the State Key Laboratory of Physical Chemistry of Solid Surface, and the Chemistry Department at Xiamen University.

Mingshu Chen

Wayne Goodman received his BS in Chemistry from Mississippi College and his PhD from the University of Texas studying with M. J. S. Dewar. After NATO postdoctoral studies in Germany and at NBS (now NIST) he joined the research staff at NBS in 1978. In 1980 he became a research scientist at Sandia National Laboratories where he served as Head of the Surface Science Division. In 1988 he joined the faculty of the Chemistry Department at Texas A&M where he is currently Distinguished Professor and Robert A. Welch Chair.

Wayne Goodman

activity for CO oxidation observed for the Au bilayer structure have aided significantly in defining the nature of the active site.[6] These ordered Au nanofilms are stable in ultrahigh vacuum (UHV) to 900 K, much higher than those temperatures, i.e. 700–800 K, where supported Au nanoparticles rapidly sinter. These studies illustrate the importance of defects on the oxide support in stabilizing Au nanoparticles and the need for designing optimum oxide supports for Au and other noble metal catalysts. This review summarises our current understanding of the origin of the unique catalytic properties of titania-supported Au catalysts for CO oxidation and is organized as follows: interaction of Au with oxide supports; active site/structure and; design and synthesis of active Au nanofilms.

2. Interaction of Au with oxide supports

2.1 Importance of surface defects

Defects on oxide surfaces play a key role in the nucleation and growth of metal nanoparticles as well as in defining their electronic and chemical properties. Therefore considerable work has focused on the characterization of surface defects and their interaction with metal atoms and particles.[5] The adsorption of probe molecules in conjunction with scanning tunneling microscopy (STM) allow the detailed characterization of surface defects. STM is especially useful in that it provides atomic-level information.[7,8] Fig. 1(A) shows a high resolution STM image of a single crystal rutile surface of

titania, specifically the TiO$_2$(110) surface.[9] The bright spots along the rows correspond to the five-coordinate Ti atom sites, i.e. the coordinately unsaturated Ti cations, as shown in the schematic of Fig. 1(B). The additional bright spots between the ordered rows are surface oxygen vacancies, so-called defects, as indicated by the red circles in Fig. 1(B). Defects of this kind can be created by sputtering with Ar$^+$ or by annealing in UHV.[8] Such defects have been found to markedly affect the adsorption energy, the particle shape, and the electronic structure of deposited Au nanoparticles and to influence their unique catalytic properties.[4–7,9–11] Theoretical calculations have demonstrated that Au particles bind more strongly to a defect-rich surface compared to a defect-deficient surface and that charge transfer may occur from the titania support to the Au particles.[7] High resolution STM combined with density functional theoretical (DFT) calculations have confirmed that bridging oxygen vacancies are the active nucleation sites for Au particles on titania, and that each vacancy site can bind approximately three Au atoms on average.[7] The adsorption energy of a single Au atom on an oxygen vacancy site is more stable by 0.45 eV compared to the stoichiometric surface. Low energy ion scattering (LEIS) has been used to examine the growth of Au on TiO$_2$(110).[10,11] Two-dimensional (2-D) Au islands are initially formed on the titania surface up to a critical coverage that depends on the defect density, after which three-dimensional (3-D) particles nucleate. The critical Au coverage at which transformation of Au particles from 2-D to 3-D occurs has been shown to be markedly dependent on the defect density, i.e. the maximum coverage of 2-D domains
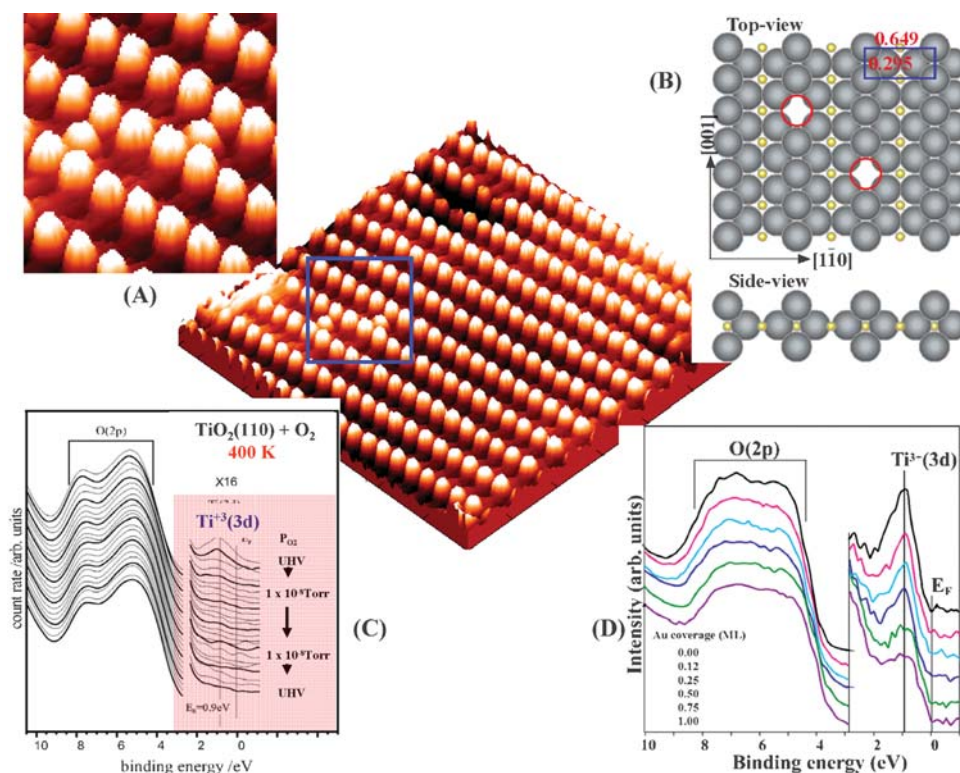

Fig. 1 (a) A high-resolution STM image of TiO$_2$(110), (b) a schematic structural model of TiO$_2$(110) with empty circles indicating the surface oxygen vacancies, (c) and (d) UPS spectra for a reduced TiO$_2$(110) surface following exposure to oxygen at 400 K and deposition of various amounts of Au at room temperature, respectively.

This journal is © The Royal Society of Chemistry 2008

Chem. Soc. Rev., 2008, 37, 1860–1870 | 1861

correlates closely with the surface defect density. Au nano-particles on defect-rich titania are found to be much more chemically active than on defect-deficient titania.[12]

Using ultraviolet photoemission spectroscopy (UPS), surface oxygen vacancies on a highly reduced titania surface have been titrated by exposure to oxygen or Au deposition in our laboratory.[9] Emission from a Ti^{3+} electronic level at a binding energy of 0.9 eV is evident in the UPS data of Fig. 1(C) and (D). Note that on an oxygen vacancy site, two neighboring Ti atoms are reduced from Ti^{4+} to Ti^{3+}. These Ti^{3+} surface defects can be completely re-oxidized by exposure to oxygen,[8,9] as shown in Fig. 1(C). Following Au deposition onto the reduced titania surface, a decrease in the intensity of the Ti^{3+} state is apparent, showing that Au initially nucleates at the defect sites.[9] This suggests that Au atoms bond to the surface at oxygen vacancy sites, i.e. bonding between Au and Ti^{3+}. The existence of Au–Ti bonds is also evident in well-ordered Au mono- and bi-layer films on a TiO_x/Mo(112) (see section 2.3)[6] and in TiO_2-supported Au nanoparticles studied with extended X-ray absorption fine structure (EXAFS).[13] In the latter, EXAFS shows a normal Au–Ti bond distance whereas the Au–O bond distance is well in excess of the normal Au–O bond length, suggesting that Au binds with Ti rather than O at the Au–oxide interface.

Fig. 2 shows STM images of <0.05 ML and 0.25 ML (1 ML: one monolayer corresponds to one Au atom per surface five-coordinate-Ti^{4+}) of Au deposited on a TiO_2(110) single crystalline surface at 300 K followed by an anneal at 850 K for 2 min.[4,9] The atomically-resolved TiO_2(110) surface consists of flat terraces with atom rows separated by ∼0.645 nm. One-dimensional (1-D) and 2-D Au nanoparticles are apparent and nucleate at defect sites at very low Au coverages. At Au coverage of 0.25 ML, Au nanoparticles with specific morphologies are imaged as bright protrusions, indicating a relatively narrow particle size distribution. Schematics of the 1-D, 2-D, and 3-D Au structures with one, two, and three atomic-layers in thickness are shown

in Fig. 2. These pictures show that Au nanoparticles initially nucleate at defect sites, growing first from 1-D to 2-D, then finally to 3-D structures.

2.2 Sintering of Au nanoparticles

Due to the intrinsic properties of Au, its interaction with most metal oxides is relatively weak, in most cases weaker than the Au–Au bond. This is demonstrated with temperature-programmed desorption (TPD) of Au in conjunction with theoretical calculations, where the binding energy of Au to an oxide support is shown to be much smaller than the Au–Au bond. These relative energy differences lead to facile sintering of Au nanoparticles as a function of reaction time, i.e. small, highly dispersed particles eventually convert to thermodynamically preferred larger particles.[4] This limitation has restricted the commercialization of supported Au nanoparticles as catalysts. Accordingly the thermal stability of oxide supported Au nanoparticles has been a subject of extensive study. It is generally agreed that the sintering of titania supported Au nanoparticles occurs mainly via the Ostwald ripening mechanism.[10] Ostwald ripening, first described by Wilhelm Ostwald in 1896, describes the energetically preferred mechanism by which large particles grow larger, drawing material from smaller particles, which shrink. This thermodynamically-driven spontaneous process occurs because larger particles are more energetically favored due to their greater volume to surface area ratio. As the system minimizes its overall energy, molecules/atoms on the surface of the smaller (energetically less favorable) particles diffuse and add to the larger particles. Therefore, the smaller particles continue to shrink, while the larger particles continue to grow. Note that particle diffusion/coalescence, where two or more particles merge to form a larger particle, may occur and even dominate under certain reaction conditions. Parker and Campbell have developed an improved kinetic model, based on the pioneering model of Wynblatt and Gjostein (WG), for
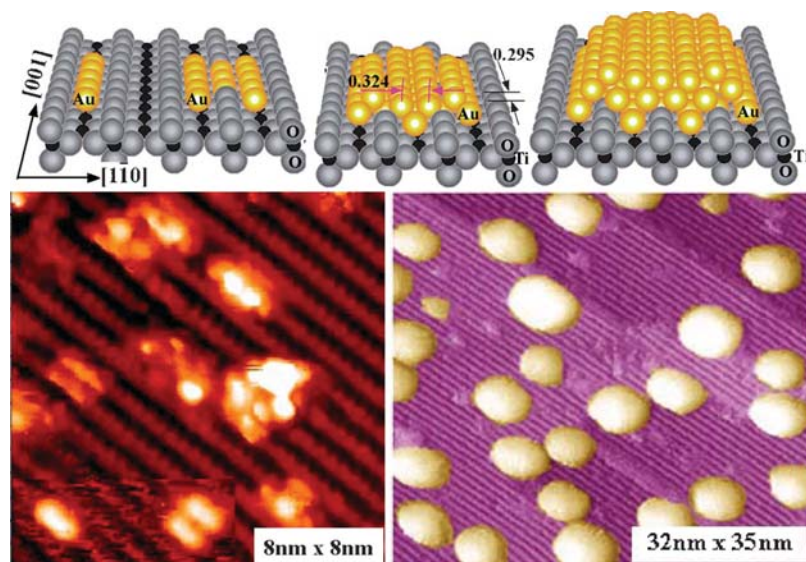

Fig. 2 Schematic structural models for 1-D, 2-D and 3-D structures with two-atomic and three-atomic-layers thick Au particles on the TiO_2(110). And STM image of Au/TiO_2(110)-(1 × 1) with a Au coverage of 0.25 ML.
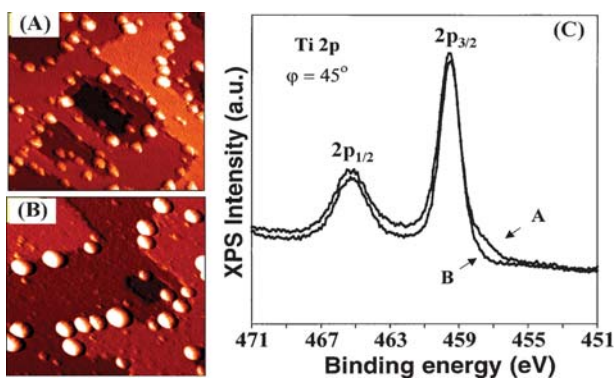
Fig. 3 STM images of Au/TiO$_2$(110)-(1 × 1) before (A) and after (B) after 120 min of CO–O$_2$ (2 : 1) exposure at 10 Torr. The Au coverage was 0.25 ML, and the sample was annealed at 850 K for 2 min before the exposures. All of the exposures are given at 300 K. The size of the images is 50 nm by 50 nm. (C) Corresponding core-level spectra (Ti 2p) measured at grazing emission, θ = 45° from the crystal normal.

the sintering of supported metal nanoparticles that can be used to more accurately predict the particle distribution as a function of reaction time.[10]

Sintering of supported Au nanoparticles was found to be significantly different under reaction conditions compared to a vacuum environment. Using STM the sintering in UHV for Au particles with a size of 2–5 nm was shown to occur above 600 K. CO exposure has no apparent effect on the morphology of the Au/TiO$_2$(110), whereas significant changes occur after exposure to O$_2$ or CO–O$_2$ at or near room temperature, as shown in Fig. 3.[4] With exposures of CO–O$_2$, the Au particle density was greatly reduced as a result of sintering. X-Ray photoemission spectra (XPS) show no changes in the chemical composition of the Au/TiO$_2$(110) surface, especially the feature corresponding to reduced titanium sites, before and after CO exposure; however, the partially reduced TiO$_2$(110) surface was oxidized after CO–O$_2$ (and O$_2$ alone, not shown) exposure (see Fig. 3). A small shoulder at the low binding energy side of the XPS Ti 2p$_{3/2}$ peak, owing to the presence of Ti^{3+} species, was completely absent after a 120 min CO–O$_2$ exposure at 300 K. Since the structural and surface chemical changes upon exposure to O$_2$ and CO–O$_2$ were identical and due to the fact that there were no detectable changes after exposure to CO, it was concluded that the Au/TiO$_2$(110) surface exhibits an exceptionally high reactivity toward O$_2$ at 300 K that promotes the sintering of the Au nanoparticles. In reaction studies, the Au nanoparticles exhibited a very high activity toward CO oxidation; however, the surface was effectively deactivated after reaction for 120 min. This deactivation is believed to be caused by O$_2$-induced agglomeration of the Au nanoparticles as seen in Fig. 3.

Recently, it was also shown that an oxidized TiO$_2$ surface can bind small Au nanoparticles (less than 20 atoms) stronger than on a reduced TiO$_2$ surface, owing to the stabilization of covalent bonds as well as ionic bonding at troughs.[14] This specific case is different from that of catalytic active Au nanoparticles with an optimum particle size of 2–3 nm (a few hundred atoms) shown to sinter more rapidly under oxidizing condition as discussed above.[4]

2.3 Design and synthesis of sinter-resist oxide supports

Because supported Au catalysts typically deactivate by sintering, considerable effort has focused on the design and synthesis of sinter-resist oxide supports, e.g. dispersion of Au nanoparticles on nano-sized oxide supports or restricted movement in oxide nanopores. An example of such a model system is a Ti-doped SiO$_2$ film prepared on a Mo single crystal surface.[9] Ti was found to incorporate into the surface forming Ti–O–Si linkages at low coverage and TiO$_x$ 3-D islands at a relatively higher coverage. Deposited Au atoms were found to nucleate primarily at Ti defects or at the extremities of TiO$_x$ islands. Due to site separation, the thermal sinter-resistance of the Au particles was greatly enhanced compared to the sintering properties of Au on SiO$_2$.

Recently a highly ordered, reduced titania surface has been synthesized on a Mo(112) substrate.[6] The film was prepared by deposition of ∼1 ML Ti onto a monolayer SiO$_2$ film that grown on Mo(112) under UHV, following subsequent oxidation in ∼5 × 10^{-8} Torr O$_2$ at 850 K, annealing at 1200 K and decomposition at 1400 K. An atomically resolved STM image, a low-energy electron diffraction (LEED) pattern, and a structural model for this reduced titania surface, designated as (8 × 2)-TiO$_x$, are shown in Fig. 4. In this model seven Ti atoms decorate every eight Mo atoms along the Mo(112) trough, binding to the surface via Ti–O–Mo bonds and to each other via Ti–O–Ti linkages. This structure is consistent with the atomically resolved STM image showing a pair of protruding Ti rows for each pair of troughs in the Mo(112) surface. Accordingly the distance between the rows of each pair is somewhat smaller than the distance between each pair of rows. This unusual feature is likely a result of the fact that the row distance of the Mo substrate along the [−110] direction is 0.445 nm, much too long for Ti–Ti bonding via a Ti–O–Ti linkage. Thus, two rows of Ti displace laterally towards each other to form an effective Ti–O–Ti bond. The Ti atom density is therefore estimated to be 7/8 of that of the top layer of Mo atoms in Mo(112). This well-ordered titania film exhibits a single phonon feature at 84 meV in high-resolution electron energy loss spectroscopy (HREELS) and
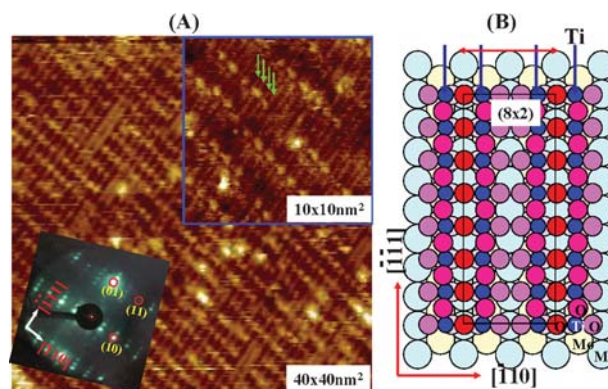

Fig. 4 (A) STM images of (8 × 2)-TiO$_x$/Mo(112), and (B) a possible structural model. U_S = +1.0 V, I = 0.5 nA. The inserts show a (8 × 2) LEED pattern and a high resolution STM image. Two pairs of arrows were shown to indicate the Ti rows in the proposed structural model and the protruding line seen in the STM image.
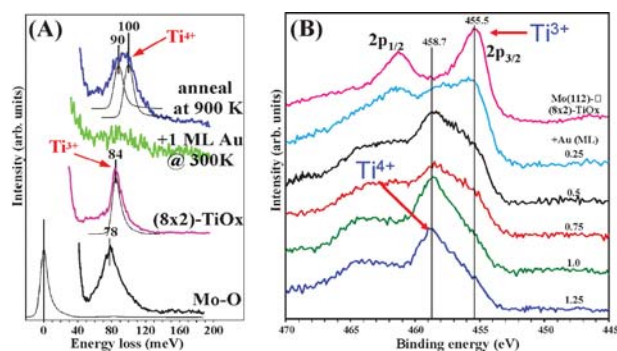
This journal is © The Royal Society of Chemistry 2008

Chem. Soc. Rev., 2008, **37**, 1860–1870 | 1863

Fig. 5 (A) HREELS spectra for the O/Mo(112), TiO$_x$/Mo(112) and Au/TiO$_x$/Mo(112) as indicated. (B) XPS Ti 2p spectra of Au on the TiO$_x$/Mo(112) at various Au coverages followed by an anneal at 900 K.

is assigned to the Ti–O stretching mode, as shown in Fig. 5(A). Considering the energy loss at 95 meV for the Ti–O stretching mode for bulk TiO$_2$, the phonon feature at 84 meV is consistent with a reduced titania film as evident from the XPS data (Fig. 5(B)).

Early studies using LEIS and STM for Au on TiO$_2$(110) have revealed that Au bonding on oxygen vacancy sites, *i.e.* reduced TiO$_2$, is stronger than the corresponding bonding to 5-fold coordinated Ti sites and bridging oxygen sites, *i.e.* a stoichiometric surface.[5,7] On the rutile TiO$_2$(110) surface (see Fig. 1(B)), the two Ti atoms nearest to an oxygen vacancy are reduced to Ti^{3+}, whereas for the (8 × 2)-TiO$_x$ thin film there is a full monolayer of reduced Ti^{3+} sites. Accordingly, strong binding between deposited Au and the TiO$_x$ surface is anticipated. Indeed, upon deposition of Au onto this (8 × 2)-TiO$_x$ surface followed by an anneal at 900 K, Au completely wets the surface as indicated by the Au/Mo AES ratio, the corresponding ν_{CO} intensity, and as evidenced by the STM images shown in Fig. 6.[6,15] The optimal annealing temperature of 900 K was obtained by monitoring the Au/Ti, Au/Mo and
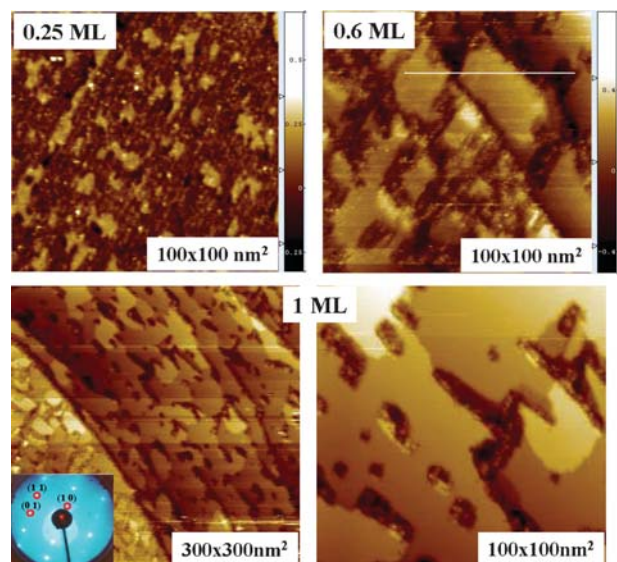
Ti/Mo AES ratio, and the related intensity of CO adsorption at 90 K as a function of annealing temperature for a ∼1 ML Au deposited onto the TiO$_x$/Mo(112) surface at room temperature. 2-D Au islands were formed initially and increase in size with an increase in Au coverage. At 1 ML, large smooth terraces were imaged without formation of 3-D particles, and a sharp (1 × 1) LEED pattern was apparent (insert of Fig. 6). The two ordered structures, (1 × 1) mono- and (1 × 3) bilayer, were formed at Au coverages of 1 and 1.3 ML. Fig. 7 shows atomically resolved images of the (1 × 1) and (1 × 3) Au films. Protruding rows with spacings of ∼4.5 and ∼13.5 Å, corresponding to one and three times the Mo(112) surface spacing along the [110] direction, are consistent with the observed (1 × 1) and (1 × 3) LEED patterns. More detailed STM images show atomically resolved arrangements of the surface atoms, consistent with the proposed structural models of Fig. 7.

The wetting of Au on this TiO$_x$ film is also evidenced by low-energy ion scattering spectroscopy (LEIS), in which the Au peak intensity increases linearly up to one monolayer, as compared with that of Au on Mo(112) (Fig. 8(A)).[15] 2-D growth of Au up to 1 ML on the TiO$_x$/Mo(112) contrasts with the growth of Au on TiO$_2$(110) where 3-D clustering occurs at a coverage >0.2 ML, demonstrating that reduced titania is indeed important in the binding of Au. The temperature-programmed desorption (TPD) of Au from TiO$_x$ is compared with the TPD of Au from Mo(112) in Fig. 8(B).[15] At sub-monolayer Au coverages, only one desorption feature of Au from TiO$_x$ is evident with a peak desorption temperature between 1260–1310 K. This peak temperature is lower than the desorption maximum of ∼1450 K for Au from Mo(112), thereby excluding the possibility of direct bonding between Au and substrate Mo atoms in the ordered Au/TiO$_x$/Mo(112) films. Upon increasing the Au coverage to greater than 1 ML, a shoulder at ∼1200 K appears, and is assigned to desorption from 3-D Au nanoparticles. These results confirm that the Au–TiO$_x$ binding energy is greater than the Au–Au binding energy, consistent with the unusual stability of these ordered Au nanofilms. The high binding energy between Au and the TiO$_x$/Mo(112) surface is the driving force for Au wetting this oxide support.

Fig. 6 STM images of various amounts of Au on (8 × 2)-TiO$_x$/Mo(112) after an anneal at 900 K. U_S = +1.0 V, I = 0.5 nA.
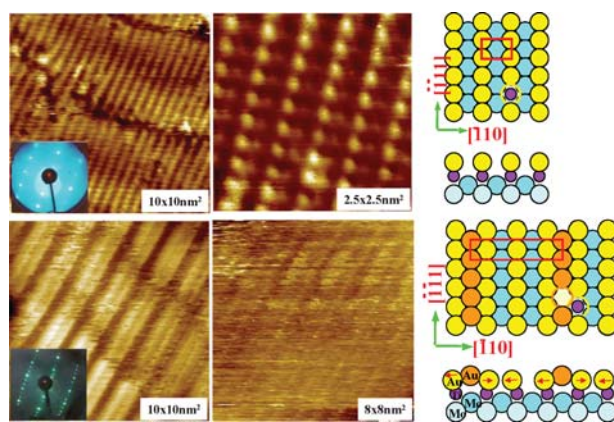

Fig. 7 Atomic resolved STM images of Mo(112)-(1 × 1)-(Au,TiO$_x$) and Mo(112)-(1 × 3)-(Au, TiO$_x$) and the corresponding structural models.
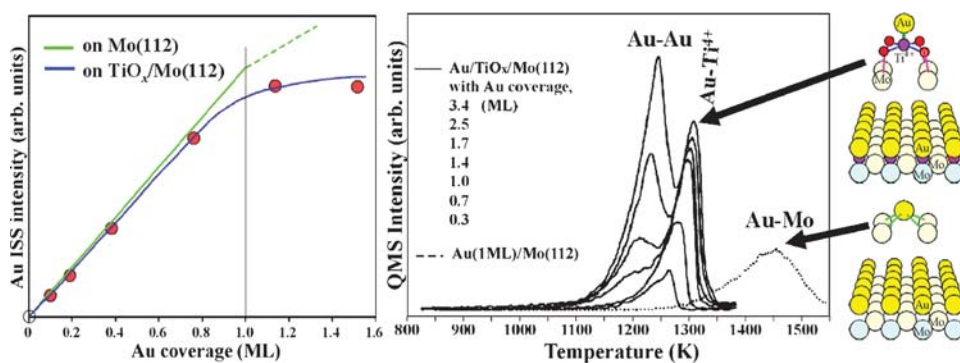
Fig. 8 (A) LEIS intensity of Au as a function of Au coverage on the TiO$_x$/Mo(112) and Mo(112). (B) TPD spectra of Au on Mo(112) with coverage of $\sim$1 ML and on TiO$_x$/Mo(112) with various Au coverages. The binding geometries of Au on the Mo(112) and TiO$_x$/Mo(112) were schematically shown for comparison.

In Fig. 6(B), the XPS Ti 2p peaks are shown for Au on the TiO$_x$ film as a function of Au coverage.[15] The Ti 2p feature for the TiO$_x$ film is apparent with a Ti 2p$_{3/2}$ binding energy (BE) at $\sim$455.7 eV. This peak position is $\sim$2.4 eV lower than 458.1 eV observed for monolayer TiO$_2$ on Mo(112) and Mo(110), and thus is assigned to Ti^{3+} states, consistent with a single phonon feature observed at 84 meV by HREELS (Fig. 6(A)). Upon deposition of Au, the Ti 2p$_{2/3}$ peak shifts markedly to a higher BE with a peak maximum at 458.8 eV, corresponding to a titanium oxidation state of 4+. Furthermore, the Ti–O phonon feature shifts from 84 to 95–100 meV, consistent with the presence of Ti^{4+} subsequent to formation of the (1 × 1) monolayer structure. A Au-induced Ti oxidation state change from Ti^{3+} in (8 × 2)-TiO$_x$/Mo(112) to Ti^{4+} in (1 × 1)-Au/TiO$_x$/Mo(112) is attributed primarily to restructuring of the TiO$_x$ film leading to changes in the coordination geometries. This observation demonstrates the strong interaction between Au and the reduced titania surface.

3. Active site structure

3.1 Structure of the active site

Catalytic activities of supported Au nanoparticles for CO oxidation are reported to be strongly dependent on the particle size, the particle shape, and the nature of the support.[2,4–6,9] From a variety of experimental observations, the corner and/ or edge sites at the perimeter/contact area of the interface between the Au nanoparticles and the support are purported to serve as unique sites for reactant activation. These results imply that higher rates should result with a decrease in particle size. However, in fact the catalytic rate decreases as the particle size decreases below 3 nm (with a thickness of two atomic layer) for supported Au nanoparticles (see Fig. 9(A)).[4,9] Moreover, a lower catalytic rate is found for the (1 × 1) monolayer compared to the rate for the (1 × 3) bilayer of Au/TiO$_x$/Mo(112) (see Fig. 9(B)).[6] These data suggest a synergism between the first and second layer is essential for the unique catalytic activity for supported Au nanoparticles. Note that the particle size required to achieve the best catalytic performance may be different in various systems due to different particle shapes, given that the more important factor is the requisite bilayer feature. Even with a similar number of Au atoms, the apparent size of a particle can vary substantially with particle morphology. For example, a Au$_{10}$ particle may be active if present as a 3-D structure, but inactive if present as planar 1-D or 2-D structures.

The rates computed on a per surface Au atom basis for CO oxidation obtained on the (1 × 3) bilayer Au nanofilm is some 45 times higher than rates reported for high-surface-area TiO$_2$ supported Au nanoparticles.[6] The rates for ordered bilayers, model nanoparticles two-atomic-layers in thickness, and the very best high-surface-area supported catalysts are compared in Fig. 10.[9] The blue bars of the histogram are the computed rates based on total Au. The rates obtained for the ordered bilayers are approximately one order of magnitude higher than the rates for the high-surface-area supported catalysts. As discussed above, assuming that the active site consists of a combination of the first and second layer Au atoms (see the inserts of Fig. 10), the rates, computed on a per active site basis from the corresponding particle structure, become comparable as shown by the red bars of the Fig. 10 histogram. It is noteworthy that on a per Au atom basis, the rates for the supported particles are decidedly lower than for the Au bilayer. This may arise due to: (1) the fact that various sizes and shapes of the particles coexist on the surface; (2) an electronic effect caused by particle contact area, particle shape, etc; and/or (3) a steric effect in that the reactants have multi-directional access to the bilayer structure but only unidirectional access to the Au nanoparticles. The importance of the interface may well be reflected from an inverse catalyst system of TiO$_2$ nanoparticles on bulk Au(111) surface studied by Rodriguez et al.,[16] in which metallic Au sites located nearby the oxide nanoparticles were shown to be the catalytically active sites.

3.2 Nature of the active site

The nature of the active site particularly with respect to whether metallic Au or positive Au, i.e. Au$^+$ and/or Au^{3+} is the active species, remains controversial. Most studies, including those using model supported catalysts, have found that metallic or slightly negative Au can be attributed to their unique catalytic activities.[2,4–7,9–12] The electronic state of Au nanoparticles can be probed using CO adsorption in combination with infrared spectroscopy.[9,17] It has been shown that the ν_{CO} mode shifts to a lower frequency on electron-rich Au clusters and to a higher
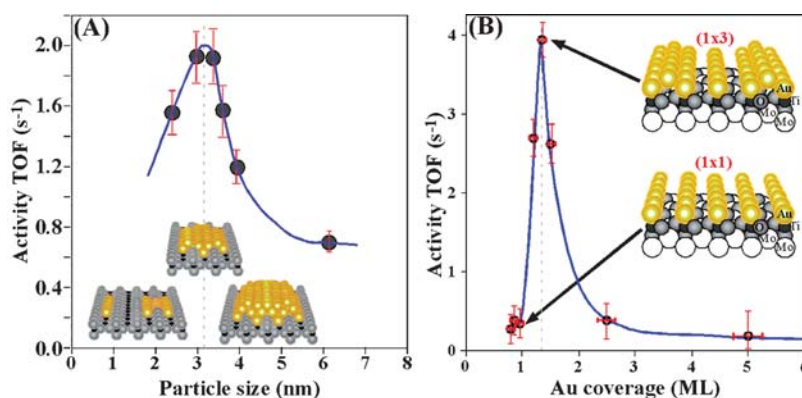
Fig. 9 Catalytic activity for CO oxidation as a function of (A) particle size on the $TiO_2(110)$, with $CO : O_2 = 1 : 5$ and a total pressure of 40 Torr, at 353 K; and (B) Au coverage on the $Mo(112)$-(8×2)-TiO_x; $CO : O_2 = 2 : 1$ and total pressure $= 5$ Torr at room temperature.
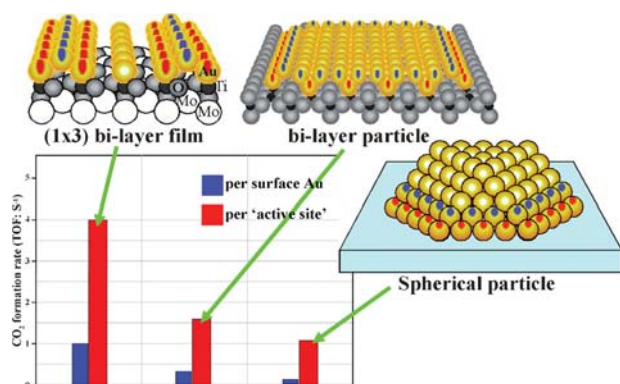

Fig. 10 Comparison of catalytic activities for CO oxidation on the $Mo(112)$-(1×3)-(Au,TiO_x), $Au/TiO_2(110)$ and Au supported on high-surface-area TiO_2 with a mean particle size of ~ 3 nm. The corresponding structural models are marked in red and blue ticks to indicate the active sites.
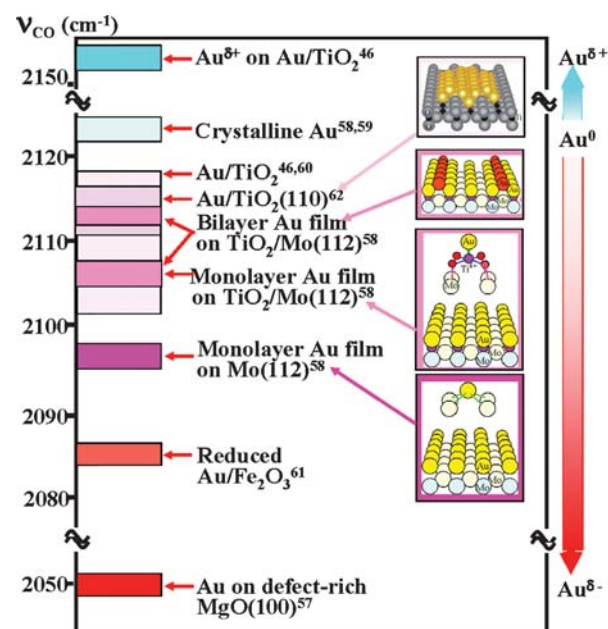

Fig. 11 Comparison of the stretching frequencies for CO adsorption on various supported Au catalysts. The components of the figure were taken from ref. 9.

frequency on electron-deficient clusters relative to bulk Au, and that the extent of the shift can be correlated with the electronic charge on Au, as shown in Fig. 11.[9] The ν_{CO} frequencies for CO adsorption on ordered Au monolayer and bilayer structures are compared with monolayer and multilayer Au on molybdenum single crystals, together with pertinent literature data, in Fig. 11. For monolayer Au on reduced titania, a single ν_{CO} mode corresponding to CO adsorbed on the a-top site of a Au atom is observed at ~ 2107 cm^{-1} for low CO exposures. For bilayer Au on reduced titania, both the first and second layer Au atoms are accessible to CO, thus a broad ν_{CO} feature at 2109 cm^{-1} is observed, a feature that can be decomposed into two bands at 2107 and 2112 cm^{-1}. These two features correspond to atop adsorbed CO on first layer Au and to CO adsorbed on second layer Au, respectively. These results suggest that CO binds more tightly to the first layer than to the second layer Au atoms. For CO adsorbed on multilayer Au, *e.g.* eight monolayers of Au on single crystal molybdenum, the ν_{CO} mode is found at 2124 cm^{-1}, a frequency identical to those found for CO on bulk crystal Au surfaces. On monolayer Au on molybdenum, where the Au has been shown to be negatively charged, the ν_{CO} mode is at 2095 cm^{-1}. The extent of the electron transfer from the substrate molybdenum to Au was estimated to be ~ 0.08

electrons based on the charge transfer reported for $Au/Mo(110)$. As displayed in Fig. 11, ν_{CO} frequencies at ~ 2124, 2112, 2107 and 2095 cm^{-1} are evident for low CO exposures on multilayer Au on molybdenum, for the second layer of Au in a Au bilayer on titania, for monolayer Au on titania, and for monolayer Au on $Mo(112)$, respectively. These observed ν_{CO} frequencies demonstrate that the Au films on reduced titania are electron-rich, *e.g.* Au$^{\delta-}$, and that the extent of electron transfer from the titania film to the Au is less than that for monolayer Au on Mo. Note that the surface arrangements of the atoms in monolayer Au on a single crystal Mo surface and monolayer Au on a reduced titania surface are similar, with the exception that in the former, Au binds directly to the substrate Mo while in the latter, Au binds to the substrate *via* Ti. This sequence of ν_{CO} frequencies, or the extent of the electron-rich state of Au, is consistent with the order of the heats of adsorption for CO, *i.e.* monolayer Au on molybdenum

> monolayer Au on titania > multilayer or bulk-like Au. The electron-rich nature of Au nanoparticles is supported by theoretical calculations and ancillary experimental data. As shown in Fig. 11, ν_{CO} frequencies are reported at 2120–2100 cm^{-1} for CO on Au particles supported on TiO$_2$, $\sim$2088 cm^{-1} for Au on Fe$_2$O$_3$ (reduced FeO), and 2050 cm^{-1} on very small Au nanoparticles supported on defect-rich MgO. In contrast, CO adsorbed on positive Au exhibits a frequency ranging from 2148 to 2210 cm^{-1}.

Electron-rich Au nanoparticles are reported to adsorb O$_2$ more strongly and to activate the O–O bond *via* charge transfer from Au by forming a superoxo-like species, and also to facilitate activation of CO.[5,9,10,18–20] Furthermore molecularly chemisorbed oxygen on Au/TiO$_2$ at the surface was found to react directly with CO to form CO$_2$ without O$_2$ dissociation. This is consistent with electron-rich Au playing a critical role in O–O bond activation, and the reaction pathway for CO oxidation on small Au particles proceeding *via* a dioxygen species rather than atomic oxygen. A direct correlation has been found between the activity of Au particles for the catalytic oxidation of CO and the concentration of F-centers (defects) at the surface of a MgO support,[21] implying a critical role of surface F-centers in the activation of Au in Au/MgO catalysts.[21,22] Moreover, an interesting evidence of that negative charged Au is more active can be seen from that Au$_6^-$ is capable of oxidizing CO at a rate 100 times greater than previously reported for model or commercial gold cluster-based catalysts.[23] Note that the gold cluster anions have undergone only a single reaction cycle at most, while a real catalyst can run over thousands of reaction cycles.

Positive Au, *e.g.* Au$^+$ and Au^{3+}, have been reported to be active for CO oxidation by several groups.[24,25] Guzman and Gates using X-ray absorption near-edge structure (XANES) investigated the oxidation state of MgO-supported Au catalysts with particle sizes of approximately 3 nm during CO oxidation.[24] With various CO : O$_2$ reactant ratios, these authors found the CO$_2$ formation rate to increase with the concentration of Au$^+$. From these data the authors proposed a critical role of Au$^+$ in supported Au catalysts for CO oxidation. It is noteworthy, however, that this conclusion was based on data where the CO : O$_2$ reactant ratio was altered significantly, a change that could dramatically effect the reaction rate. For example, for CO catalytic oxidation on platinum-group metals, CO$_2$ formation is positive first order with respect to the O$_2$ partial pressure, with extremely high rates realized for oxygen-rich reaction conditions.[26] Furthermore, the observed rate of $\sim$2 $\times$ 10^{-3} s^{-1} over MgO-supported Au particles by Guzman and Gates[24] is far lower than rates found for active metallic Au nanoparticles.[9] Hutchings *et al.* investigated the oxidation states of Au in α-Fe$_2$O$_3$-supported Au catalysts for CO oxidation using X-ray photoelectron, X-ray absorption, and Mössbauer effect spectroscopies.[25] These authors found that 5% wt Au/Fe$_2$O$_3$ prepared by co-precipitation of the respective hydroxides and drying at 393 K exhibits a high rate for CO oxidation, whereas a catalyst calcined at 673 K in air exhibits a relatively low rate. The former catalyst was determined to contain mainly cationic Au with a mean particle size from 3.8 to 7 nm, while the latter catalyst contained primarily metallic Au with a mean particle

size of 8.2 nm. Hutchings *et al.* concluded that cationic Au may assist metallic Au in catalytic CO oxidation, but these authors could not conclude that metallic Au is inactive or that cationic Au is present in active Au catalysts. It has been demonstrated that the activity of supported Au catalysts strongly depends on the particle size, with the best performance achieved at approximately 3 nm. The activity decreases dramatically with an increase in particle size as shown by Haruta *et al.* and Goodman *et al.*[2,4–6,9] A metallic Au particle of 8.2 nm intrinsically has a very low catalytic activity. It is noteworthy that in the Hutchings's experiments,[25] on a 50 mg 5% wt Au/Fe$_2$O$_3$ a CO flow rate of 0.5 ml min^{-1}, 100% conversion corresponds to a TOF of approximately 2 $\times$ 10^{-3} (per Au site per second), a rate far lower than 0.1–4 observed for metallic Au catalysts.[2,4–6,9]

Very recently, using similar techniques, Gates *et al.*[13] investigated FeO$_x$ doped Au/TiO$_2$ (Degussa P25) for CO oxidation using XANES and EXAFS. The transient XANES data recorded in flowing CO–O$_2$ show that cationic Au was rapidly reduced completely to zero-valent Au under CO oxidation conditions. These results provide strong evidence for the presence of zero-valent Au rather than cationic Au in the working catalysts. Note a specific rate of approximately 0.1 CO$_2$ molecule per Au site per second was achieved in this system, a rate comparable to the rates reported for other oxide supported Au catalysts.[2,5,9] In fact, Friend's group[27] have shown that CO can react with atomic oxygen on a Au surface at 70 K, which is consistent with Au$^+$ and Au^{3+} being strong oxidizers that could potentially oxidize CO, *i.e.* be reduced by CO, at very low temperatures. Schwartz *et al.*[28] also showed that a higher catalytic rate correlates with fully reduced Au, and that after reduction no re-oxidation was observed under CO oxidation conditions, even in air at temperatures as high as 300 °C. Using X-ray adsorption spectroscopy (XAS) combined with XPS and FTIR, Kung *et al.*[29] concluded that for a Au/TiO$_2$ catalyst, metallic Au is necessary for high CO catalytic oxidation rates. With XANES and ^{13}C isotopic transient analysis, Davis *et al.*[30] also concluded that active Au/TiO$_2$ and Au/Al$_2$O$_3$ catalysts contain predominately metallic Au. Altogether, this body of data shows that although cationic Au may be active for CO catalytic oxidation, its activity is decidedly lower than the activity of metallic Au nanoparticles.

3.3 Reaction pathway

Another relevant question is whether the support is involved directly in activating the reactant molecules. It is generally agreed that the support plays an important role in stabilizing and defining the morphologies and electronic properties of Au nanoparticles.[5,9] The perimeter/contact area of the interface between the Au particles and the support has been proposed to serve as a unique reaction site where reactants are activated. From theoretical calculations, the support has been shown to play an active role in the bonding and activation of adsorbates bound to Au.[18] Molina and Hammer have proposed the active site to be low-coordinated Au atoms in combination with surface cations interacting simultaneously with an adsorbate.[31]
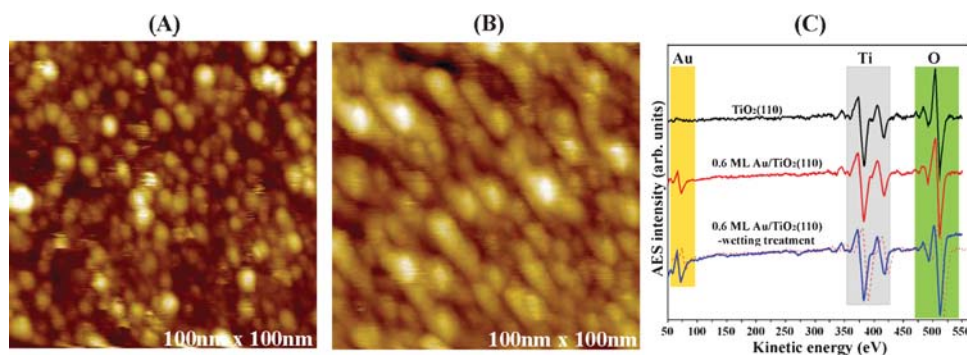
This journal is © The Royal Society of Chemistry 2008

Chem. Soc. Rev., 2008, **37**, 1860–1870 | 1867

Fig. 12 STM images of 0.6 ML Au on a reduced $TiO_2(110)$, (A) before and (B) after reduction treatments, and (C) the corresponding AES spectra, showing an apparent increase of Au intensity after reduction treatments.

The Au–TiO_2 interface and Au itself have been proposed for activation of the O_2 molecule. Model catalytic studies for Au on $TiO_2(110)$ and $TiO_x/Mo(112)$ demonstrated that a bilayer structure is critical to the unique catalytic properties of Au for CO oxidation.[4,6,9] Under UHV conditions, the active Au nanoparticle and/or nanofilms were found to be electron-rich, *i.e.* negatively charged. Furthermore in the ordered Au monolayer and bilayer structures described above, the $Ti^{\delta+}$ of the support titania is not assessable to the reactants, since each surface Ti site binds directly to Au atoms located at the topmost surface.[6] The exceptionally high catalytic activities for CO oxidation observed on ordered bilayer Au thus strongly suggest a Au-only CO oxidation pathway, *i.e.* that the oxide support itself may not need to directly involve the activation/reaction of reactant molecules. This reaction pathway is supported by recent DFT calculations that show the reaction sequence for CO oxidation for Au-only surface sites on a TiO_2 supported Au nanoparticle to have a similar activation energy (0.36–0.40 eV) as that involving the support.[32] Moreover, molecularly chemisorbed oxygen on Au/TiO_2 is found to be stable at the surface[19] and to react directly with CO to form CO_2 without requiring dissociation of O_2.[20]

Using *in situ* XANES van Bokhoven *et al.*[33] found clear evidence for charge transfer from small Au particles to oxygen along with partial depletion of the Au d band upon exposure to oxygen. This leads to partially oxidized Au particles that can be reduced quickly by CO to CO_2. Under CO oxidation reaction conditions, CO is dominant on the surface, consistent with O_2 being activated on Au particles rather than the support. The results also imply that partially oxidized Au is present as a short-lived species under catalytic conditions. This also suggests that the rate-limiting step for CO oxidation on supported Au catalysts is the activation of O_2. The first layer Au on $TiO_2(110)$ surface was found to bind oxygen 40% more strongly than do Au particles using temperature-programmed desorption (TPD).[10]

4. Design and synthesis of active Au nanofilms

The unique activities of highly dispersed nano-sized Au particles on oxide surfaces are found to strongly correlate with the Au particle size, *e.g.* the highest turnover frequency (TOF, reaction rate per surface Au site per second) occurs at a particle size of

~3 nm. On a model catalytic system, Au/$TiO_2(110)$, a similar trend in catalytic activity was observed under realistic reaction conditions. The maximum reaction rate, a turnover frequency of 2, was observed for a surface with Au particles of a mean particle size of ~3 nm and a particle thickness of two atomic layers as determined by STM. Regarding the facts of facile sintering of supported Au nanoparticles, gold nanoparticles with a size of 2–5 nm were introduced into silica mesopores[34] and α-Fe_2O_3 nanopores,[35] anticipated to have higher sinter-resistance. The ordered Au bilayer nanofilm supported on a $TiO_x/Mo(112)$ is highly active for CO oxidation. This rate is 1–2 orders of magnitude higher than rates reported for high-surface-area supported catalysts. This confirms that a bilayer feature is critical for the unique catalytic properties and demonstrates that a reduced oxide-supported Au nanofilm is more active even than supported Au nanoparticles. Compared to supported metal nanoparticles, a nanofilm catalyst enhances the density of the surface active sites from 2–3 orders of magnitude. Moreover, the surface active sites are well-defined and can greatly improve selectivity.

On a reduced $SrTiO_3$-(2 × 1) surface, Silly and Castell[36] found that below 573 K Au forms metastable 2-D islands with one atomic layer thickness up to a coverage of 0.75 ML. In our laboratory, recent results[37] show that Au wets to a greater extent on both planar and high-surface-area TiO_2 surfaces following thorough reduction. As shown in Fig. 12, upon deposition of 0.6 ML Au onto a highly reduced $TiO_2(110)$ surface followed by reduction, enhanced wetting by Au was apparent by STM imaging (Fig. 12(A) and (B)), and by the increase in the related Au AES intensity (Fig. 12(C)). Another case in point is the wetting by Au of a TiO_x modified magnesium oxide support[38] where a monolayer thickness TiO_x film was grown on a MgO(100) surface. These Au nanofilms have been shown to exhibit significantly higher catalytic activities and stabilities, even to the extent of being potential commercial catalysts.[37,38]

Conclusions

The strong dependence of the particle sizes for supported Au nanoparticles, particularly the loss of catalytic activity with an increase in particle size above 6–10 nm, requires extreme stability under reaction conditions for commercialization. Well-ordered Au bilayer nanofilms on a reduced titania thin film exhibit a catalytic activity comparable to the most active

Au nanoparticles, *i.e.* the thickness of the particle rather than the particle diameter is the critical structural feature with respect to catalytic activity. These studies have shown that a bilayer Au structure is a critical feature for catalytically active Au nanoparticles, along with low coordinated Au sites, support-to-particle charge transfer effects, and quantum size effects. The strong binding between Au and a reduced titania surface results in complete wetting by Au nanofilms of an oxide surface. The so formed Au bilayer nanofilm (two atomic layers in thickness) exhibits unusual high activity for CO oxidation, and increases the active site density by 1–3 orders of magnitude compared to typical high-surface-area supported Au catalysts. Cationic Au may be an active catalytic species, however the activity of these sites are lower than that of metallic Au nanoparticles. Future studies should focus on the details of the sintering mechanism and the design/synthesis of functional oxide supports to enhance the gold-support interaction and to retard particle sintering.

Acknowledgements

References

1 G. C. Bond, P. A. Sermon, G. Webb, D. A. Buchanan and P. B. Wells, Hydrogenation over supported Au catalysts, *J. Chem. Soc., Chem. Commun.*, 1973, 444.

2 M. Haruta, T. Kobayashi, H. Sano and N. Yamada, Novel Au catalysts for the oxidation of carbon-monoxide at a temperature far below 0-degrees-C, *Chem. Lett.*, 1987, **2**, 405.

3 A. S. K. Hashmi and G. J. Hutchings, Au catalysis, *Angew. Chem., Int. Ed.*, 2006, **45**, 7896, and references cited therein.

4 M. Valden, X. Lai and D. W. Goodman, Onset of catalytic activity of Au clusters on titania with the appearance of nonmetallic properties, *Science*, 1998, **281**, 1647.

5 M. S. Chen and D. W. Goodman, Structure–activity relationships in supported Au catalysts, *Catal. Today*, 2006, **111**, 22, and references cited therein.

6 M. S. Chen and D. W. Goodman, The structure of catalytically active Au on titania, *Science*, 2004, **306**, 252.

7 E. Wahlstrom, N. Lopez, R. Schaub, P. Thostrup, A. Ronnau, C. Africh, E. Laegsgaard, J. K. Norskov and F. Besenbacher, Bonding of Au nanoparticles to oxygen vacancies on rutile TiO$_2$(110), *Phys. Rev. Lett.*, 2003, **90**, 026101.

8 M. A. Henderson, W. S. Epling, C. L. Perkins, C. H. F. Peden and U. Diebold, Interaction of molecular oxygen with the vacuum-annealed TiO$_2$(110) surface: Molecular and dissociative channels, *J. Phys. Chem. B*, 1999, **103**, 5328.

9 M. S. Chen and D. W. Goodman, Catalytically active Au: from nano-particles to ultra-thin films, *Acc. Chem. Res.*, 2006, **39**, 739, and references cited therein.

10 S. C. Parker and C. T. Campbell, Reactivity and sintering kinetics of Au/TiO$_2$(110) model catalysts: particle size effects, *Top. Catal.*, 2007, **44**, 3, and references cited therein.

11 F. Cosandey and T. E. Madey, Growth, morphology, interfacial effects and catalytic properties of Au on TiO$_2$, *Surf. Rev. Lett.*, 2001, **8**, 73.

12 J. A. Rodriguez, G. Liu, T. Jirsak, J. Hrbek, Z. P. Chang, J. Dvorak and A. Maiti, Activation of Au on titania: Adsorption and reaction of SO$_2$ on Au/TiO$_2$(110), *J. Am. Chem. Soc.*, 2002, **124**, 5242.

13 S. Carrettin, Y. Hao, V. Aguilar-Guerrero, B. C. Gates, S. Trasobares, J. J. Calvino and A. Corma, Increasing the number of oxygen vacancies on TiO$_2$ by doping with iron increases the activity of supported Au for CO oxidation, *Chem.–Eur. J.*, 2007, **13**, 7771.

14 D. Matthey, J. G. Wang, S. Wendt, J. Matthiesen, R. Schaub, E. Laegsgaard, B. Hammer and F. Besenbacher, Enhanced bonding of Au nanoparticles on oxidized TiO$_2$(110), *Science*, 2007, **315**, 1692.

15 M. S. Chen, K. Luo, D. Kumar, C. W. Yi and D. W. Goodman, The structure of ordered Au films on TiO$_x$, *Surf. Sci.*, 2007, **601**, 632.

16 J. A. Rodriguez, S. Ma, P. Liu, J. Hrbek, J. Evans and M. Pérez, Activity of CeO$_x$ and TiO$_x$ nanoparticles grown on Au(111) in the water-gas shift reaction, *Science*, 2007, **318**, 1757.

17 M. Chen, Y. Cai, Z. Yan and D. W. Goodman, On the origin of the unique properties of supported Au bilayers, *J. Am. Chem. Soc.*, 2006, **128**, 6341.

18 N. Lopez, T. V. W. Janssens, B. S. Clausen, Y. Xu, M. Mavrikakis, T. Bligaard and J. K. Norskov, On the origin of the catalytic activity of Au nanoparticles for low-temperature CO oxidation, *J. Catal.*, 2004, **223**, 232.

19 D. Stolcic, M. Fischer, G. Gantefor, Y. D. Kim, Q. Sun and P. Jena, Direct observation of key reaction intermediates on Au particles, *J. Am. Chem. Soc.*, 2003, **125**, 2848.

20 J. D. Stiehl, T. S. Kim, S. M. McClure and C. B. Mullins, Reaction of CO with molecularly chemisorbed oxygen on TiO$_2$-supported Au nanoparticles, *J. Am. Chem. Soc.*, 2004, **126** 13574.

21 Z. Yan, S. Chinta, A. A. Mohamed, J. P. Fackler, Jr and D. W. Goodman, The Role of F-Centers in Catalysis by Au Supported on MgO, *J. Am. Chem. Soc.*, 2005, **127**, 1604.

22 M. Sterrer, M. Yulikov, E. Fischbach, M. Heyde, H. P. Rust, G. Pacchioni, T. Risse and H. J. Freund, Interaction of Au clusters with color centers on MgO(001) films, *Angew. Chem., Int. Ed.*, 2006, **45**, 2630.

23 W. T. Wallace and R. L. Whetten, Coadsorption of CO and O$_2$ on selected gold clusters: Evidence for efficient room-temperature CO$_2$ generation, *J. Am. Chem. Soc.*, 2002, **124**, 7499.

24 J. Guzman and B. C. Gates, Catalysis by supported Au: Correlation between catalytic activity for CO oxidation and oxidation states of Au, *J. Am. Chem. Soc.*, 2004, **126**, 2672.

25 G. J. Hutchings, M. S. Hall, A. F. Carley, P. London, B. E. Solsona, C. J. Kiely, A. Herzing, M. Makkee, J. A. Moulijn, A. Overweg, J. C. Fierro-Gonzalez, J. Guzman and B. C. Gates, Role of Au cations in the oxidation of carbon monoxide catalyzed by iron oxide-supported Au, *J. Catal.*, 2006, **242**, 71, and references cited therein.

26 M. S. Chen, Y. Cai, Z. Yan, K. K. Gath, S. Axnanda and D. W. Goodman, "Highly active surfaces for CO oxidation on Rh, Pd, and Pt", *Surf. Sci.*, 2007, **601**, 5326, and references cited therein.

27 B. K. Min, A. R. Alemozafar, D. Pinnaduwage, X. Deng and C. M. Friend, Efficient CO oxidation at low temperature on Au(111), *J. Phys. Chem. B*, 2006, **110**, 19833.

28 V. Schwartz, D. R. Mullins, W. Yan, B. Chen, S. Dai and S. H. Overbury, XAS study of Au supported on TiO2: Influence of oxidation state and particle size on catalytic activity, *J. Phys. Chem. B*, 2004, **108**, 15782.

29 J. H. Yang, J. D. Henao, M. C. Raphulu, Y. Wang, T. Caputo, A. J. Groszek, M. C. Kung, M. S. Scurrel, J. T. Miller and H. H. Kung, Activation of Au/TiO$_2$ catalyst for CO oxidation, *J. Phys. Chem. B*, 2005, **109**, 10319.

30 J. T. Calla, M. T. Bore, A. K. Datye and R. J. Davis, Effect of alumina and titania on the oxidation of CO over Au nanoparticles evaluated by C-13 isotopic transient analysis, *J. Catal.*, 2006, **238**, 458.

31 L. M. Molina and B. Hammer, Active role of oxide support during CO oxidation at Au/MgO, *Phys. Rev. Lett.*, 2003, **90**, 206102.

32 I. N. Remediakis, N. Lopez and J. K. Norskov, CO oxidation on rutile-supported Au nanoparticles, *Angew. Chem., Int. Ed.*, 2005, **44**, 1824.

33 J. A. van Bokhoven, C. Louis, J. Miller, M. Tromp, O. V. Safonova and P. Glatzel, Activation of oxygen on Au/alumina catalysts: *In situ* high-energy-resolution fluorescence and time-resolved X-ray spectroscopy, *Angew. Chem., Int. Ed.*, 2006, **45**, 4651.

34 A. Fukuoka, H. Araki, J. Kimura, Y. Sakamoto, T. Higuchi, N. Sugimoto, S. Inagaki and M. Ichikawa, Template synthesis of

nanoparticle arrays of gold, platinum and palladium in mesoporous silica films and powders, *J. Mater. Chem.*, 2004, **14**, 752, and references cited therein.

35 Z. Zhong, J. Ho, J. Teo, S. Shen and A. Gedanken, Synthesis of porous alpha-Fe$_2$O$_3$ nanorods and deposition of very small gold particles in the pores for catalytic oxidation of CO, *Chem. Mater.*, 2007, **19**, 4776.

36 F. Silly and M. R. Castell, Bimodal growth of Au on SrTiO$_3$(001), *Phys. Rev. Lett.*, 2006, **96**, 086104.

37 M. S. Chen and D. W. Goodman, *Synthesis of highly active Au catalysts on titania*, to be published.

38 S. Axnanda, M. S. Chen and D. W. Goodman, *Growth and catalytic properties of ultra-thin Au films on TiO supported on MgO(100)*, to be published.